Surface Melt-Induced Acceleration of Greenland Ice-Sheet Flow
H. Jay Zwally, *et al.*
Science **297**, 218 (2002);
DOI: 10.1126/science.1072708

affected by NR manipulation. Infusion of AP5 selectively into the hippocampus impairs spatial memory acquisition but shows no effect on retrieval of previously trained spatial reference memory in the water maze (*37*), suggesting that our results reflect a primary deficit in NR-dependent memory formation in CA3 that is then revealed as a deficit in recall under limited cue conditions.

A substantial proportion of aged individuals exhibit deficits of memory recall (*38*). In early Alzheimer patients, retrieval is the first type of memory function to decline; such retrieval deficits may serve as an early predictor of Alzheimer disease (*39, 40*). Normal aging produces a CA3-selective pattern of neurochemical alterations (*41–43*). Exposure to chronic stress, which can lead to memory deficits, also selectively causes atrophy in the apical dendrites of CA3 pyramidal cells (*44*). These results are consistent with our findings in mice that the CA3 region is critical for cognitive functions related to memory recall through pattern completion.

This study along with our previous study with CA1-NR1 KO mice (*15*, *24*) illustrates the power of cell type-restricted, adult-onset gene manipulations in the study of molecular, cellular, and neuronal circuitry mechanisms underlying cognition. The same neurotransmitter receptors (i.e., NMDA receptors) can play distinct roles in the mnemonic process depending on where and in which neural circuitry in the hippocampus they are expressed. It is expected that other genetically engineered mice with precise spatial and/or temporal specificity will help dissect mechanisms for a variety of cognitive functions.

References and Notes

1. J. O'Keefe, L. Nadel, *The Hippocampus as a Cognitive Map* (Clarendon Press, Oxford, UK, 1978).
2. L. R. Squire, *Psychol. Rev.* **99**, 195 (1992).
3. D. G. Amaral, M. P. Witter, *Neuroscience* **31**, 571 (1989).
4. N. Ishizuka, J. Weber, D. G. Amaral, *J. Comp. Neurol.* **295**, 580 (1990).
5. D. Marr, *Philos. Trans. R. Soc. London Ser. B* **262**, 23 (1971).
6. A. R. Gardner-Medwin, *Proc. R. Soc. London Ser. B* **194**, 375 (1976).
7. J. J. Hopfield, *Proc. Natl. Acad. Sci. U.S.A.* **79**, 2554 (1982).
8. B. L. McNaughton, R. G. M. Morris, *Trends Neurosci.* **10**, 408 (1987).
9. E. T. Rolls, in *The Computing Neuron*, R. Durbin, C. Miall, G. Mitchison, Eds. (Addison-Wesley, Wokingham, UK, 1989), pp. 125–159.
10. M. E. Hasselmo, E. Schnell, E. Barkai, *J. Neurosci.* **15**, 5249 (1995).
11. E. W. Harris, C. W. Cotman, *Neurosci. Lett.* **70**, 132 (1986).
12. S. Williams, D. Johnston, *Science* **242**, 84 (1988).
13. R. A. Zalutsky, R. A. Nicoll, *Science* **248**, 1619 (1990).
14. T. W. Berger, M. F. Yeckel, in *Long-Term Potentiation: A Debate of Current Issues*, M. Baudry, J. L. Davis, Eds. (MIT Press, Cambridge, MA, 1991), pp. 327–356.
15. J. Z. Tsien, P. T. Huerta, S. Tonegawa, *Cell* **87**, 1327 (1996).
16. W. Wisden, P. H. Seeburg, *J. Neurosci.* **14**, 3582 (1993).
17. Relevant data and experimental procedures can be found at *Science* Online.
18. Y. Liu, N. Fujise, T. Kosaka, *Exp. Brain Res.* **108**, 389 (1996).
19. M. Watanabe *et al.*, unpublished data.
20. S. Chattarji, B. S. S. Rao, K. Nakazawa, S. Tonegawa, unpublished data.
21. R. G. M. Morris, P. Garrud, J. N. P. Rawlins, J. O'Keefe, *Nature* **297**, 681 (1982).
22. R. Muller, *Neuron* **17**, 813 (1996).
23. P. J. Best, A. M. White, A. Minai, *Annu. Rev. Neurosci.* **24**, 459 (2001).
24. T. J. McHugh, K. I. Blum, T. Z. Tsien, S. Tonegawa, M. A. Wilson, *Cell* **87**, 1339 (1996).
25. R. U. Muller, J. L. Kubie, *J. Neurosci.* **7**, 1951 (1987).
26. M. C. Quirk, K. I. Blum, M. A. Wilson, *J. Neurosci.* **21**, 240 (2001).
27. P. A. Schwartzkroin, D. A. Prince, *Brain Res.* **147**, 117 (1978).
28. R. K. S. Wong, R. D. Traub, *J. Neurophysiol.* **49**, 442 (1983).
29. O. Paulsen, E. I. Moser, *Trends Neurosci.* **21**, 273 (1998).
30. G. Buzsaki, *Prog. Neurobiol.* **22**, 131 (1984).
31. S. J. Y. Mizumori, C. A. Barnes, B. L. McNaughton, *Brain Res.* **50**, 99 (1989).
32. J. Csicsvari, H. Hirase, A. Czurko, G. Buzsaki, *Neuron* **21**, 179 (1998).
33. S. J. Y. Mizumori, B. L. McNaughton, C. A. Barnes, F. B. Fox, *J. Neurosci.* **9**, 3915 (1989).
34. J. O'Keefe, D. H. Conway, *Exp. Brain Res.* **31**, 573 (1978).
35. P. A. Hetherington, M. L. Shapiro, *Behav. Neurosci.* **111**, 20 (1997).
36. N. N. Urban, D. A. Henze, G. Barrionuevo, *Hippocampus* **11**, 408 (2001).
37. R. G. M. Morris, *J. Neurosci.* **9**, 3040 (1989).
38. M. Gallagher, P. R. Rapp, *Annu. Rev. Psychol.* **48**, 339 (1997).
39. H. Tuokko, R. Vernon-Wilkinson, J. Weir, B. L. Beattie, *J. Clin. Exp. Neuropsychol.* **13**, 871 (1991).
40. L. Backman, *et al.*, *Neurology* **52**, 1861 (1999).
41. H. Le Jeune, D. Cecyre, W. Rowe, M. J. Meaney, R. Quirion, *Neuroscience* **74**, 349 (1996).
42. T. Kadar, S. Dachir, B. Shukitt-Hale, A. Levy, *J. Neural Transm.* **105**, 987 (1998).
43. M. M. Adams *et al.*, *J. Comp. Neurol.* **432**, 230 (2001).
44. B. S. McEwen, *Annu. Rev. Neurosci.* **22**, 105 (1999).

45. We thank P. Soriano, F. Tronche, T. Furukawa, R. J. DiLeone, F. Bushard, S. Chattarji, and M. Fukaya for reagents, assistance, and/or advice. We also thank the many members of the Tonegawa and Wilson Labs for valuable advice and discussions. Supported by an NIH grant RO1-NS32925 (S.T.), RIKEN (S.T. and M.W.), NIH grant P50-MH58880 (S.T. and M.W.), HHMI (S.T.), and Human Frontier Science Program (K.N.).

Supporting Online Material
www.sciencemag.org/cgi/content/full/1071795/DC1
Materials and Methods
Fig. S1

12 March 2002; accepted 17 May 2002
Published online 30 May 2002;
10.1126/science.1071795
Include this information when citing this paper.

Surface Melt–Induced Acceleration of Greenland Ice-Sheet Flow

H. Jay Zwally,[1]* Waleed Abdalati,[2] Tom Herring,[3] Kristine Larson,[4] Jack Saba,[5] Konrad Steffen[6]

Ice flow at a location in the equilibrium zone of the west-central Greenland Ice Sheet accelerates above the midwinter average rate during periods of summer melting. The near coincidence of the ice acceleration with the duration of surface melting, followed by deceleration after the melting ceases, indicates that glacial sliding is enhanced by rapid migration of surface meltwater to the ice-bedrock interface. Interannual variations in the ice acceleration are correlated with variations in the intensity of the surface melting, with larger increases accompanying higher amounts of summer melting. The indicated coupling between surface melting and ice-sheet flow provides a mechanism for rapid, large-scale, dynamic responses of ice sheets to climate warming.

The time scale for dynamic responses of ice sheets to changes in climate (e.g., snow accumulation and surface temperature) is typically considered to be hundreds to thousands of years (*1*). Because most ice-sheet motion occurs by ice deformation in the lower layers, basal sliding, or deformation in basal till, the effects of changes in surface climate must be transmitted deep into the ice to affect the ice flow markedly. In particular, changes in the surface-mass balance alter the ice thickness slowly, and therefore the driving stresses in the deforming layers, as thickness changes accumulate. Changes in surface temperature can also affect the rate of ice deformation or basal sliding, but only after the very slow conduction of heat to the lower layers (*2*). In contrast to the flow of grounded ice, both floating glacier tongues (*3*) and Antarctic ice

[1]Oceans and Ice Branch, Code 971, NASA Goddard Space Flight Center, Greenbelt, MD 20771, USA. [2]Code YS, NASA Headquarters, 300 E Street, SW, Washington, DC 20546, USA. [3]Department of Earth, Atmospheric, and Planetary Sciences, MIT Room 54-618, 77 Massachusetts Avenue, Cambridge, MA 02139, USA. [4]Department of Aerospace Engineering Sciences, University of Colorado, Boulder, CO 80309, USA. [5]Raytheon Inc., Code 971, NASA Goddard Space Flight Center, Greenbelt, MD 20771, USA. [6]CIRES, University of Colorado, CB 216, Boulder, CO 80309, USA.

*To whom correspondence should be addressed. E-mail: jay.zwally@gsfc.nasa.gov

shelves (*4*) respond quickly to changes in basal heat fluxes and melting, as well as to the effects of surface meltwater trapping in crevasses. Although the transfer of surface meltwater to the base of a grounded ice sheet can provide a rapid mechanism for transferring heat and lubricating fluid to the bottom, this mechanism has not been given much consideration in studies of ice-sheet dynamics. In particular, the Greenland Ice Sheet is grounded above sea level and is generally believed to respond gradually to climate warming (*5*, *6*), mainly by melting at the surface.

Increases in ice velocity occur in alpine glaciers during periods of surface melt in summer (*7*–*9*) and have also been observed in Greenland outlet glaciers (*10*–*12*). For example, Bindschadler *et al*. (*8*) measured a velocity increase from 10 cm/day in winter to 12 cm/day in summer in the Variegated Glacier, a surge-type glacier in Alaska. However, short-term velocity variations have not been observed in the flow of ice sheets away from ice streams and outlet glaciers. Even inland of the fast-flowing Jakobshavn Isbrae in west-central Greenland, seasonal variations were not found (*13*).

Velocity and Melt Observations

To examine the possibility of seasonal or interannual changes in ice-sheet flow, we initiated year-round global positioning system (GPS) measurements at the Swiss Camp (*14*, *15*) at 1175 m (69.57°N, 49.31°W) near the equilibrium line (*16*) in west-central Greenland in June 1996 (Fig. 1). The camp is about 35 km from the ice edge and about 510 km downstream from the ice divide. Characteristic glaciological features of the region are illustrated in Fig. 2. The ice thickness at the camp is 1220 m (*17*), and a numerical thermodynamic-dynamic ice model suggests that the basal temperature is at the pressure-melting point (PMP) of –1.0°C (*18*). The horizontal ice velocity is nearly constant from the surface to the lower boundary layer, where ice shearing occurs. For basal ice at the PMP, part of the surface velocity is typically from ice sliding at the base, but the magnitude of sliding is difficult to estimate without borehole measurements (*19*).

Our ice velocities are derived from GPS-measured positions of a 4-m pole embedded 2 m in the ice beginning in June 1996 (*20*). The receiver recorded automatically for 12-hour periods at intervals of 10 or 15 days (*21*). GPS data were analyzed using GAMIT and GLOBK software (*22*). To examine changes in ice velocity with respect to the direction of ice flow, a smoothed line of motion was derived as a function of time. The time series of north and east positions [N(t), E(t)] were each fitted to parabolas as a function of time (t). The direction of motion was computed from the derivatives (dN/dE = dN/dt /dE/dt) and is approximately a linear function of time. The derived direction of motion is toward the southwest at an azimuth of 234.963°E on 1 January 1997 and curving toward the west at the rate of 0.106°/year. Although most of the motion is along-track, systematic cross-track displacements up to about ±20 cm occur annually, as discussed below.

Figure 3 shows the horizontal along-track velocity from June 1996 through mid-November 1999. Data from periods during the winter months with little or no change in velocity were used to compute a constant base velocity of 31.33 ± 0.02 cm/day (*23*). In 1996, the velocity increased slightly from the winter value to a maximum of 32.8 cm/day on August 9, and then returned to the winter value. A small temporary increase to 32.8 cm/day also occurred in March of 1997. In subsequent summers, the velocity increased markedly to a maximum of

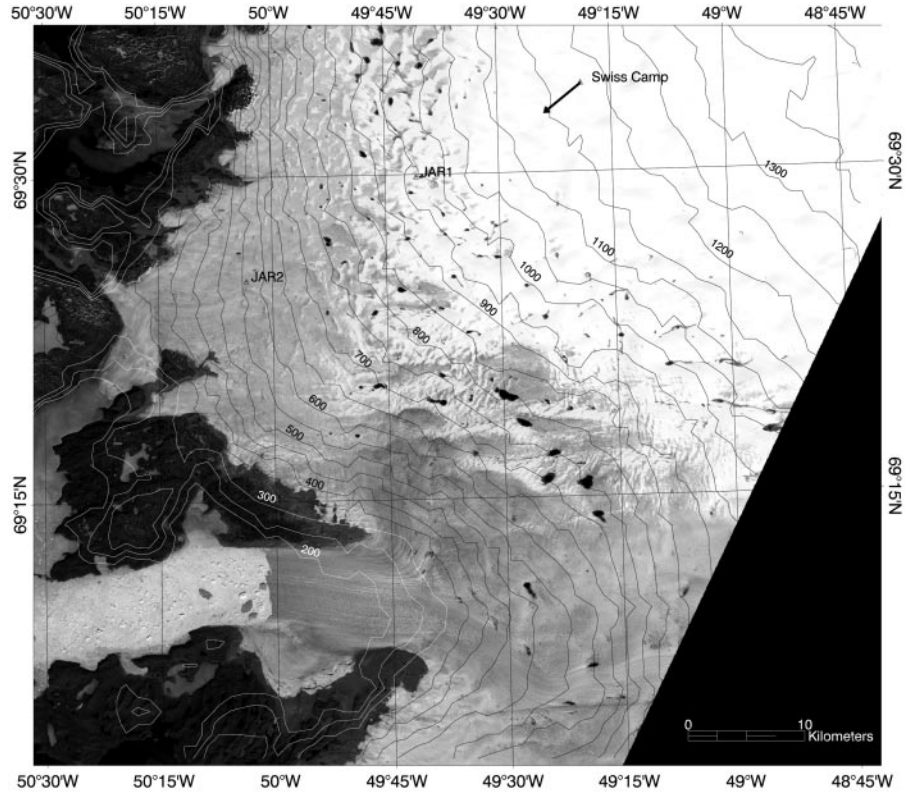

Fig. 1. Elevation contours (50 m) on a Landsat Thematic Mapper image (channel 3) taken on 22 June 1990, which is typically about one-third of the way through the melt season. Locations of the Swiss Camp and the Automated Weather Station at JAR-1 and JAR-2 are marked. The indicated flowline direction of 235°E at the camp curves westward toward the grounded ice edge. The grayer areas at lower elevations in the image are bare ice, with some whiter patches of remaining winter snow near the ice-snow line. By the end of the melt season in late August to early September, the firn-ice boundary usually retreats to around the average location of the equilibrium line (*15*) near the Swiss Camp. The dark patches are melt lakes, some of which show dark lines of inflow channels. Later in the season, melt lakes also form above the equilibrium line. Jacobshavn Isbrae is in the lower part.

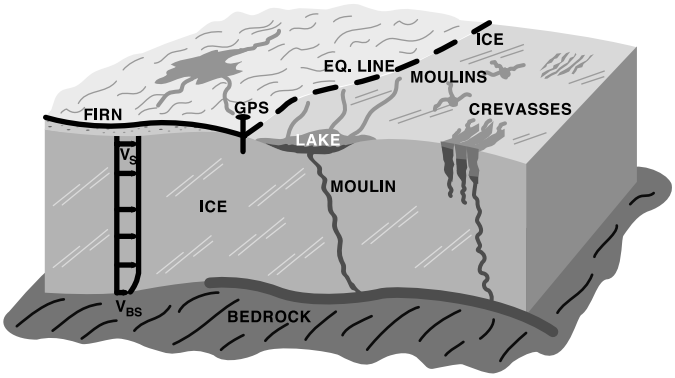

Fig. 2. Schematic of glaciological features in the equilibrium and ablation zones, including surface lakes, inflow channels, crevasses, and moulins. Ice flow for basal ice at the pressure melting point is partly from basal sliding and partly from shear deformation, which is mostly in a near-basal boundary layer.

35.1 cm/day around 9 August 1997, of 40.1 cm/day around 10 July 1998, and of 38.6 cm/day around 30 July 1999. After these periods of accelerating flow, the velocity decreased markedly to a minimum of 28.9 cm/day around 18 September 1997, of 29.8 cm/day around 19 August 1998, and of the lowest value of 27.6 cm/day around 29 August 1999. After the velocity minima, the ice slowly accelerated again over several fall months to return to the midwinter values.

The cumulative additional motion (Fig. 3) caused by the summer accelerations was computed as the difference between the measured positions and the calculated along-track positions that would have occurred under a constant velocity of 31.33 cm/day. At the transition from accelerating flow to decelerating flow in early September 1997, the ice had moved an additional 3.0 m relative to the baseline rate. At the 1998 and 1999 transitions, the respective net additional displacements were 4.7 m and 6.0 m. During periods of slower flow in the fall, after the transitions, the additional displacement was reduced by about 45 to 65% (*24*).

From a 21-year record of Greenland surface melting from passive microwave data, the summer of 1996 was the second-lowest melt year since 1979, the summer of 1997 was slightly below the 21-year average, and the summers of 1998 and 1999 were well above average (*25*). We investigated relationships between the availability of summer meltwater for basal lubrication and changes in the ice velocity using the cumulative positive degree-days (PDDs) (*26*) at the camp, as shown in Fig. 3C. For the four summers (1996 to 1999), the respective total PDDs were 47.6, 60.8, 116.5, and 94.7. The corresponding mean areas of melt from June through September in the Jacobshavn region from passive microwave data were 28.2, 52.0, 79.6, and 74.5 $\times$ 10^3 km^2, which show similar year-to-year variations as the PDDs (*27*). The quality of PDDs as an indicator of ablation and consequent meltwater production was shown by Braithwaite and Olesen (*28*), who obtained a 0.96 correlation coefficient between annual ice ablation and PDDs, even though variations in radiation and other energy-balance factors such as wind speed also affect the rate of ice ablation (*29*).

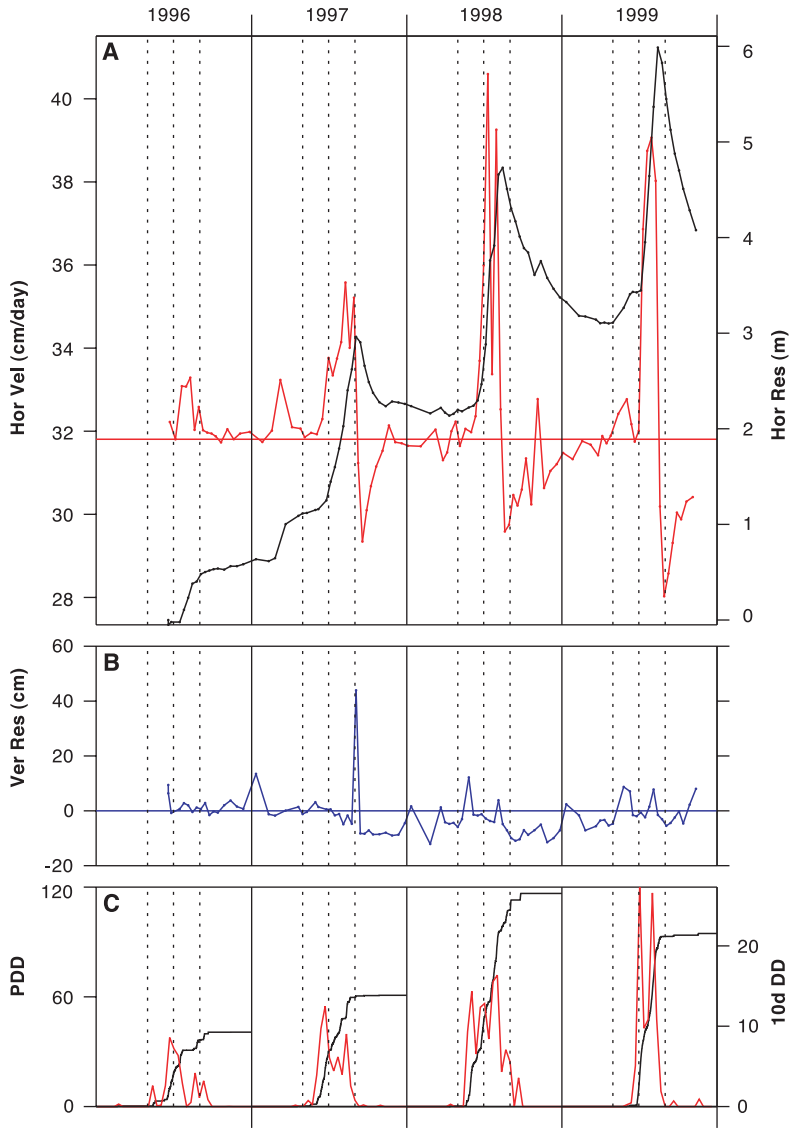

Fig. 3. (**A**) Horizontal ice velocity (red curve) along a smoothed line of motion showing ice accelerations during the summer melt seasons and the abrupt transitions to deceleration around the times of melt cessation. The cumulative additional motion (horizontal residual, black) relative to a wintertime-average velocity of 31.33 cm/day is 6.0 m by the time of the maximum velocity in 1999. (**B**) The vertical residual (blue) indicates a 50-cm uplift at the time of the 1997 transition from accelerating flow to decelerating flow. (**C**) Cumulative PDDs and PDDs for 10-day intervals (10d DD, red) from temperatures measured at the Swiss Camp, showing correlations of the melting with the intensity and timing of the ice accelerations and decelerations (units are degree-days). Vertical dotted lines mark May 1, July 1, and September 1 for each year.

Correlations Between Acceleration and Surface Melting

In all years, correlations are evident between the changes in ice velocity and both the intensities and timings of surface melting. For the summers of 1998 and 1999, the respective ratios of the increases in velocity of 8.8 and 7.3 cm/day to the PDDs of 116.5 and 94.7 are nearly the same (0.076 and 0.077), whereas the ratios in 1996 and 1997 are somewhat smaller (0.032 and 0.063). For the summer of 1999, the melting period was shorter in duration, but of greater intensity in the month of July than in the other summers.

Although melting downstream of the equilibrium line begins a few days to several weeks earlier than at the camp, comparison of the timing of the acceleration and melting is based on the melt record at the camp (*30*). Although some melting usually occurs in May, more-continuous melting does not usually begin until the beginning of June. In 1997, the onsets of ice acceleration and melting were nearly simultaneous in mid-June. In 1998, the acceleration onset (also in mid-June) lagged the melting onset by about 2 weeks. In 1999, although a small temporary increase in velocity appeared in May, the major ice acceleration and the melting onset were both delayed until the beginning of July. Correlations between the timing of the transitions from acceleration to deceleration and the cessations of melting were also good, particularly in 1997 and 1999 when the respective transitions at the beginning of September and mid-August were nearly coincident with the end of melting. In 1998, some melting continued after the transition in early August. In 1996, the year of minimal acceleration, the ice accelerated in July and early August until the end of a period of minimal melting in late August when the transition to deceleration occurred.

Acceleration Mechanism

In the ablation zone of Greenland, surface meltwater runs along the surface and collects in surface lakes or flows directly into moulins (Fig. 2). Although the internal or subglacial pathways for transit of the meltwater to the margins are generally not known, Thomsen *et al*. (*29*) assumed that water flowing into moulins quickly flows to the bottom and drains subglacially. Whether the drainage pathways tend to be vertical and channel meltwater to the base of the ice sheet, or tend to be horizontal and remain englacial, markedly affects the local availability of water for basal lubrication. One indication that the water flow is largely subglacial, at least near the margins, is that the meltwater primarily leaves the ice sheet in subglacial streams, and not in surface flow over the ice edges. Theoretically, water-filled crevasses are expected to propagate to the bottom due to the over-burden pressure of water, as compared to ice (*31*), and could provide numerous pathways for meltwater drainage throughout the ablation zone and for the initiation of moulins. Mapping of moulins and surface lakes (*29*) in the ablation zone below the camp shows that the areal density of moulins is about 0.2 moulins/km^2 and most moulins are not associated with the less-numerous surface lakes.

Therefore, flow of meltwater through moulins, and perhaps through the numerous crevasses throughout the ablation zone, is likely to provide a widespread and continual drainage from the surface to the ice base during the melt season. The surface lakes usually drain during summer, but their drainage tends to be episodic, depending on the irregular timing of the opening of drainage channels from the lakes (*15*, *32*). We believe that the observed correlations between the changes in ice velocity and the timing and intensity of the surface melting show that there is widespread and continual drainage of meltwater from the surface to the ice-sheet base during summer ablation. Because the ice base is at the PMP (*18*), a wet base maintained by basal melting is expected to be a normal condition throughout the year. Water may be maintained during winter in subglacial conduits that expand during periods of increased water pressure and accelerated flow (*33*). The probable cause of the summer acceleration is an increase in the water pressure at the bedrock interface, which is a well-known mechanism for velocity variations in alpine glaciers. For example, Iken *et al*. (*33*) found that the summer increase in subglacial water pressure actually raised the glacier by as much as 0.6 m and partially decoupled the ice from the bed. The horizontal velocity increased by three to six times and was largest at times of maximum upward velocity.

The magnitude of the acceleration at the Swiss Camp was small in the low-melt year of 1996 and increased in later years as the melting increased. Apparently, more meltwater produces larger accelerations, and the timings of melting and acceleration are closely related. The ice accelerations commenced a few weeks after the onset of melting. Later, the transition from accelerating to decelerating ice flow occurred near the cessation or slowing of melting at the end of the melt season. The short time between melt onset and acceleration, as well as the close timing between the transition and the ending of ablation, suggests that storage of meltwater after production is not an important factor affecting the acceleration.

The rapid ice deceleration after the peak velocity is reached could be associated with an increase in basal friction and reduced basal sliding caused by changes at the ice-bedrock interface that occur during the period of increased water flow. As noted above, the ice decelerates to velocities about 10% below the average winter velocity before returning to the winter velocity in late fall. This suggests that the basal sliding gradually recovers to normal winter values. Presumably, the ice acceleration begins in the lower elevations of the ablation zone, with changes in basal sliding, and propagates upstream past the Swiss Camp as sliding increases. The process of deceleration is likely to be a combination of changes in basal sliding and the dynamic response of the ice to the changing patterns of driving stresses during acceleration.

In early September 1997, during the one GPS measurement period just at the transition from accelerating to decelerating flow, the vertical residuals show a 50-cm uplift of the ice sheet (Fig. 3A). Around the time of the 1998 and 1999 transitions, the excursions of the vertical position were $<$10 cm, which is on the order of other occasional excursions in the data throughout the year. The 50-cm uplift in the 1997 data could be indicative of changes in the basal water pressure similar to that in small glaciers (*34*), or of dynamic effects in the ice occurring as the ice flow at the camp changes from accelerating to decelerating.

Around the time of the maximum accelerations in 1997, 1998, and 1999, the direction of the ice motion changed by about 1° to the right (more westward) over about 30 to 45 days, as shown by 15- to 20-cm cross-track displacements. The peak cross-track velocities are 0.5 to 1 cm/day to the right. After the rightward displacement, an equal displacement to the left slowly occurs until the next summer. These changes in direction are in addition to the 0.106°/year average rotation to the right of the smoothed line of motion. The change in direction during the acceleration could be indicative of changes in the basal friction and the ratio of the sliding velocity to the velocity from ice deformation.

Conclusions

The interaction among warmer summer temperatures, increased surface meltwater production, water flow to the base, and increased basal sliding provides a mechanism for rapid response of the ice sheets to climate change. In general, a direct coupling between increased surface melting and ice-sheet flow has been given little or no consideration in estimates of ice-sheet response to climate change (*35*). In addition to the direct effect of increased water pressure on the basal sliding, the flow of surface water at approximately 0°C to basal ice, at the PMP of –1.0°C, transfers heat for additional basal melting. The occurrence of this melt-driven acceleration in the equilibrium zone implies that the mechanism may be occurring throughout much of the ablation zone of the ice sheet, or at least where the basal temperature is at the PMP. Therefore, the rate of retreat of the ice-sheet margin under climate warming is probably faster than predicted by estimates based only on the direct increase in surface ablation (*36*). Enhanced basal sliding from surface meltwater may have contributed to the rapid demise of the Laurentide Ice Sheet during increased summer insolation and surface ablation circa 10,000 years ago (*37*) and to extensive melting of the Greenland Ice Sheet during the last interglacial (*38*), by causing a faster flow of ice to the margins, an increase in the thinning rate, and more rapid inward migration of the ablation zone.

References and Notes

1. R. B. Alley, I. M. Whillans, *J. Geophys. Res.* **89**, 6487 (1984).
2. Another long-term dynamic-response mechanism is caused by variation in the dust impurities in snowfall that affects the ice hardness, so the upper layers of Holecene ice with lower dust content are harder than the lower layers of ice-age ice with higher dust content (*39*).
3. E. Rignot, W. B. Krabill, S. P. Gogineni, I. Joughin, *J. Geophys. Res.* **106**, 34007 (2001).
4. T. Scambos, C. Hulbe, M. Fahnestock, J. Bohlander, *J. Glaciol.* **46**, 516 (2000).
5. C. Ritz, A. Fabre, A. Letreguilly, *Clim. Dyn.* **13**, 11 (1997).
6. P. Huybrechts, J. de Wolde, *J. Clim.* **12**, 2169 (1999).
7. A. Iken, *Z. Gletscherkd. Glazialgeol.* **13**, 23 (1978).
8. R. Bindschadler, W. D. Harrison, C. F. Raymond, R. Crosson, *J. Glaciol.* **18**, 181 (1977).
9. G. H. Gudmundsson *et al*., *Ann. Glaciol.* **31**, 63 (2000).
10. N. Reeh and O. B. Olesen (*40*) found summer velocity fluctuations of 15% on time scales of 2 to 10 days in the Daugaard-Jensen Glacier, an outlet glacier on the east coast of Greenland. Also, an observed 50% velocity increase for about 7.5 hours was inferred to be the result of a subglacial increase in water pressure caused by the drainage of an ice-dammed lake.
11. I. Joughin, S. Tulaczyk, M. Fahnestock, and R. Kwok (*41*) found a threefold velocity increase during the 1995 melt season in the Ryder outlet glacier in northwest Greenland, which they described as a short-lived mini-surge.
12. On Storstrommen Glacier in northeast Greenland, GPS-determined velocities for summer are generally greater than winter velocities and annual averages (*42*).
13. K. Echelmeyer, W. D. Harrison, *J. Glaciol.* **36**, 82 (1990).
14. K. Steffen, J. E. Box, *J. Geophys. Res.* **106**, 33951 (2001).
15. A. Ohmura *et al*., *ETH Greenland Expedition Progress Report No. 1* (Department of Geography, ETH, Zurich, Switzerland, 1991).
16. The equilibrium line is defined as the boundary be-

tween annual net ice accumulation and net ablation at the surface and is located at the upper elevation of bare ice (without refrozen firn or superimposed ice) at the end of the summer melt season. The empirical equation for the equilibrium-line altitude (ELA) is a decreasing quadratic function of latitude (*43*) that gives an ELA of 1418 m at the latitude of the Swiss Camp. The camp was established in 1990 at the nominal location of the equilibrium line, based on surface observations in previous years (*29*). It lies on a small ridge, and local variations in the altitude of the equilibrium zone range from around 1200 m at the camp to 1400 m south of the camp.
17. Measured by University of Kansas ice-penetrating radar. Data are available online at http://torna-do.rsl.ku.edu/1998thick.htm.
18. W. L. Wang, H. J. Zwally, W. Abdalati, S. Luo, *Ann. Glaciol*., in press, using the measured ice thickness of 1220 m. The modeled basal temperature is slightly below the PMP at the ice divide and is essentially at the PMP along a flowline from 400 km above the camp to the ice edge.
19. M. Luthi, M. Funk, A. Iken, S. Gogineni, M. Truffer, *J. Glaciol*., in press, obtained a ratio of basal sliding of 60% in the lateral shear zone of Jakobshavn Isbrae, but noted that such a high ratio is probably not representative for the ice sheet.
20. GPS data were recorded by a geodetic-quality dual-frequency Trimble 4000 SSi receiver (Trimble, Sunnyvale, CA), which is inside an insulated box in a camp tent and powered by four to six 100–a-h batteries and two 18-W solar panels. The 2-m extension of the antenna above the ice keeps the antenna above the seasonal snow accumulation, which ranges from about 0.5 to 1.8 m interannually. Yearly data were downloaded when the camp was occupied each May. Data collection ended in the fall of 1999 because of anomalous behavior of the receiver.
21. During the spring occupation of the Swiss Camp, data were usually recorded continuously instead of once every 10 to 15 days. To avoid large velocity errors for short time intervals, the following position data for multiple 12-hour time periods were averaged: 23 to 29 May 1998 (13 periods), 23 to 28 May 1999 (10 periods), and 9 and 10 June 1999 (4 periods).
22. R. W. King, *Documentation of the GAMIT GPS Analysis Software Version 10.05* (2001); and T. A. Herring, *Documentation of the GLOBK Software Version 5.1* (2001), MIT, Cambridge, MA. See also http://www-gpsg.mit.edu/~simon/gtgk. The Cartesian coordinates of the antenna were calculated, relative to bedrock sites at Thule Air Force Base, Kellyville, and Kulusuk in Greenland, from 12-hour increments of data. The average standard deviations of the coordinates calculated with GLOBK is 1.2 cm horizontally and 3.3 cm vertically. The standard deviations of the north and east components of the positions are somewhat higher during the winter periods (e.g., the standard deviation of the north component went from a base value of about 0.5 cm to a high of nearly 6 cm during the winter of 1999). The large uncertainties occurred on days when only the bedrock site at Thule was operating and when less than 12 hours of data were recorded at Swiss Camp. Times assigned to the points are the midpoints of the times of the data increments. The overall average standard deviation of the horizontal velocity is 0.14 cm/day. Analysis techniques are also described in (*44*).
23. The horizontal velocity at markers 2.15 km downstream from Swiss Camp is 0.67 cm/day slower than at the camp. Therefore, as the camp moved from 1996 to 1999, the estimated decrease in horizontal velocity was 0.036 cm/day/year, or 0.14 cm/day during the 4-year period.
24. The respective advancements and reductions for 1997, 1998, and 1999 were: 1.8 and 0.8 m, 2.5 and 1.6 m, and 2.9 and 1.9 m.
25. W. Abdalati, K. Steffen, *J. Geophys. Res.* **106**, 33983 (2001).
26. PDD = $\sum_i \alpha_i T_i/24$, where T_i are hourly averaged near-suface air temperatures, $\alpha_i = 1$ if $T_i > 0$, and $\alpha_i = 0$ if $T_i \leq 0$.
27. The year-to-year ratios of cumulative PDDs to melt areas (*19*) differ from unity by less than 19%. The Jacobshavn melt region is defined from about 65.5 to 76°N and from the western ice edge to the divide. The respective cumulative melt-days obtained from passive microwave for the area near the camp are 30, 60, 97, and 47. The year-to-year correspondence for the camp location is not as good (ratios differ from unity by up to 33%), probably because the passive-microwave index of melt days records only the occurrence of surface melting, whereas the deg-days index registers more for warm days (e.g., 5 times more for +5°C) than for days that are just above the melting point. In contrast, the melt-area index used for the Jacobshavn region is also sensitive to the intensity of melting, which expands the area of melting to higher elevations.
28. R. J. Braithwaite, O. B. Olesen, in *Glacier Fluctuations and Climate Change*, J. Oerlemans, Ed. (Kluwer, Dordrecht, Netherlands, 1989), pp. 219–233.
29. H. H. Thomsen, L. Thorning, R. J. Braithwaite, *Glacier-Hydrological Conditions on the Inland Ice North-East of Jakobshavn/Ilusissat, West Greenland: Report 138* (Gronlands Geologiske Undersogelse, Copenhagen, Denmark, 1998).
30. For example, data for 1997 through 1999 from the Automated Weather Station (AWS) (*15*) at JAR-1 at a 960-m elevation and 16.3 km downstream from the camp show that the lag in melting onset between the sites varies from only 1 to 14 days until about 30 deg-days are cumulated. The end of melting may occur even closer in time at different elevations in the ablation zone. In 1999 at least, the cessation was almost simultaneous at Swiss Camp, JAR-1, and JAR-2, which is at a 528-m elevation and 17.1 km downstream from JAR-1.
31. G. de Q. Robin, *J. Glaciol.* **13**, 543 (1974).
32. At the JAR-1 AWS site, which was located near the side of a lake hundreds of meters in diameter, the sonic surface-height data show that the surface level dropped 1.5 m in a few hours on 17 July 1996 as the water drained from the ice. A similar drop of 0.8 m occurred on 25 June 1997, when the station had moved 70 m closer to the lake edge.
33. A. Iken, H. Rothlisberger, A. Flotron, W. Haberli, *J. Glaciol.* **29**, 28 (1983).
34. C. F. Raymond, *J. Geophys. Res.* **92**, 9121 (1987).
35. J. T. Houghton *et al.*, Eds., *Climate Change 2001: The Scientific Basis* (IPCC Report, Cambridge, UK, 2001).
36. R. J. Braithwaite, O. B. Olesen, *Ann. Glaciol.* **14,** 20 (1990).
37. P. U. Clark, R. B. Alley, D. Pollard, *Science* **286**, 1103 (1999).
38. R. M. Koerner, *Science* **244**, 964 (1989).
39. N. Reeh, *Nature* **317**, 797 (1985).
40. _____, O. B. Olesen, *Ann. Glaciol.* **8**, 146 (1986).
41. I. Joughin, S. Tulaczyk, M. Fahnestock, R. Kwok, *Science* **274**, 228 (1996).
42. J. J. Mohr, N. Reeh, S. Madsen, *Nature* **391**, 273 (1998).
43. H. J. Zwally, M. B. Giovinetto, *J. Geophys. Res.* **106**, 33717 (2001).
44. K. Larson, J. Plumb, J. Zwally, W. Abdalati, *Polar. Geogr.* **25**, 22 (2002).
45. Supported by NASA's ICESat (Ice Cloud and Land Elevation Satellite) science activities and Cryospheric Sciences Program.

9 April 2002; accepted 30 May 2002
Published online 6 June 2002;
10.1126/science.1072708
Include this information when citing this paper.

Super ENSO and Global Climate Oscillations at Millennial Time Scales

Lowell Stott,[1]* Christopher Poulsen,[1] Steve Lund,[1] Robert Thunell[2]

The late Pleistocene history of seawater temperature and salinity variability in the western tropical Pacific warm pool is reconstructed from oxygen isotope ($\delta^{18}O$) and magnesium/calcium composition of planktonic foraminifera. Differentiating the calcite $\delta^{18}O$ record into components of temperature and local water $\delta^{18}O$ reveals a dominant salinity signal that varied in accord with Dansgaard/Oeschger cycles over Greenland. Salinities were higher at times of high-latitude cooling and were lower during interstadials. The pattern and magnitude of the salinity variations imply shifts in the tropical Pacific ocean/atmosphere system analogous to modern El Niño–Southern Oscillation (ENSO). El Niño conditions correlate with stadials at high latitudes, whereas La Niña conditions correlate with interstadials. Millennial-scale shifts in atmospheric convection away from the western tropical Pacific may explain many paleo-observations, including lower atmospheric CO_2, N_2O, and CH_4 during stadials and patterns of extratropical ocean variability that have tropical source functions that are negatively correlated with El Niño.

The discovery that the Earth experiences large, abrupt climate variations that have no clear external (solar) forcing has stimulated the pursuit of highly resolvable climate archives such as ice, marine, and terrestrial deposits that can provide clues about the origin of these rapid climate events. Until recently, too few records existed from the tropics to establish whether millennial climate variability is inherently tied to tropical climate dynamics. This void is being filled with new sediment cores collected by the IMAGES program (*1*).

[1]Department of Earth Sciences, University of Southern California, 3651 Trousdale Parkway, Los Angeles, CA 90089, USA. [2]Department of Geological Science, University of South Carolina, 700 Sumter Street, Columbia, SC 29208, USA.

*To whom correspondence should be addressed. E-mail: stott@usc.edu